J|A|C|S ARTICLES

Published on Web 01/29/2010

CASSCF Molecular Orbital Calculations Reveal a Purely Pseudopericyclic Mechanism for a [3,3] Sigmatropic Rearrangement

Lila Forte, Marie C. Lafortune, Irena R. Bierzynski, and James A. Duncan*

Department of Chemistry, Lewis & Clark College, Portland, Oregon 97219-7899

Received August 14, 2009; E-mail: duncan@lclark.edu

Abstract: A comparative CASSCF/6-31G*-level computational study of the concerted [3,3] sigmatropic rearrangements of *cis*-1-iminyl-2-ketenylcyclopropane (**15**), *cis*-1-iminyl-2-propadienylcyclopropane (**17**), and *cis*-1-iminyl-2-keteniminylcyclopropane (**19**) to give products **16**, **18**, and **20**, respectively, was conducted. Analysis of the active space MOs of $\mathbf{TS_{15\rightarrow16}}$, $\mathbf{TS_{17\rightarrow18}}$, and $\mathbf{TS_{19\rightarrow20}}$ suggests that the **17** → **18** and **19** → **20** rearrangements are classically pericyclic, whereas the **15** → **16** rearrangement is pseudopericyclic with two orbital disconnections—one involving the nitrogen lone-pair orbital and the other the carbonyl carbon of the ketene moiety. The novel $\mathbf{TS_{15\rightarrow16}}$ was also found to have a highly planar, tight, geometry, whereas $\mathbf{TS_{17\rightarrow18}}$ and $\mathbf{TS_{19\rightarrow20}}$ were both shown to have the boat-shaped geometry expected for classically pericyclic [3,3] sigmatropic rearrangements. Results of calculations on the [3,3] sigmatropic rearrangements involving additional transition structures, $\mathbf{TS_{21\rightarrow22}}$, $\mathbf{TS_{23\rightarrow24}}$, $\mathbf{TS_{25\rightarrow26}}$, $\mathbf{TS_{27\rightarrow28}}$, $\mathbf{TS_{29\rightarrow30}}$, and $\mathbf{TS_{31\rightarrow32}}$, demonstrate the relative uniqueness of the pseudopericyclic one, $\mathbf{TS_{15\rightarrow16}}$.

Introduction

All of the five recognized types of pericyclic reactions—electrocyclic, cycloaddition, cheletropic, sigmatropic, and group transfers/elimination—appear to have been studied with respect to possible pseudopericyclic versions.[1,2] In many cases, and particularly in the electrocyclic case,[2] the reactions appear to lack purely pseudopericyclic character. Recently, Birney has argued that in cases where both pericyclic and pseudopericyclic orbital topologies are possible, some transition structures may result from the mixing of the two electronic states.[1d] Some of these studies have relied on magnetic and NBO analyses[2e] or tools such as electron flucuation,[2f] the electron localization function (ELF),[2g] or the ellipticity of the electron density.[2h]

Inasmuch as the definition of pseudopericyclic reactions incorporates the notion of one or more orbital disconnections in a cyclic array of interacting orbitals, we have primarily used a localized orbital method, the active space orbitals derived from Complete Active Space Self Consistent Field (CASSCF) calculations, in our study of them. In the case of the [3,3] sigmatropic (Cope) rearrangement of *syn*-allenylnorbornene (**1**) to triene **2**, CASSCF/6-31G* calculations revealed that one of two transition structures leading to biradical intermediate **3** involved an orbital disconnection at the center carbon of the allene (cf. $\mathbf{TS_{1\rightarrow3}}$ in Figure 1).[3] This result would have qualified the rearrangement as being pseudopericyclic had the reaction been concerted; since it was not, we termed it an "augmented" Cope rearrangement.

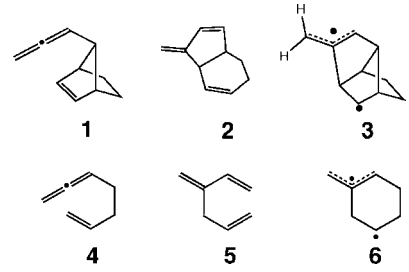

Shown in Figure 1 are two of the active space MOs that resulted from the optimization of $\mathbf{TS_{1\rightarrow3}}$. As can clearly be seen, the forming σ-bond involves overlap of the *terminal* π-orbital of the allenyl moiety with the π-orbital of the norbornene ring (Figure 1a), while the *internal* π-orbital remains intact (Figure 1b). Alternatively, the comparable active space MOs calculated for $\mathbf{TS_{4\rightarrow6}}$, involved in the Cope rearrangement of 1,2,6-heptatriene (**4**) to triene **5**, through biradical **6** shows that it is the *internal* π-orbital that is used for bonding (Figure 1c) while

(1) (a) Ross, J. A.; Seiders, R. P.; Lemal, D. M. *J. Am. Chem. Soc.* **1976**, *98*, 4325–4327. (b) Birney, D. M.; Wagenseller, P. E. *J. Am. Chem. Soc.* **1994**, *116*, 6262–6270. (c) Birney, D. M.; Ham, S.; Unruh, G. R. *J. Am. Chem. Soc.* **1997**, *119*, 4509–4517. (d) Ji, H.; Xu, X.; Ham, S.; Hammad, L. A.; Birney, D. M. *J. Am. Chem. Soc.* **2009**, *131*, 528–537, and references therein.

(2) (a) Duncan, J. A.; Calkins, D. E. G.; Chavarha, M. *J. Am. Chem. Soc.* **2008**, *130*, 6740–6748. (b) Rodríguez-Otero, J.; Cabaleiro-Lago, E.; García-López, R.; Peña-Gallego, A.; Hermida-Ramón, J. *Chem.—Eur. J.* **2005**, *11*, 5966–5974. (c) Rodríguez-Otero, J.; Cabaleiro-Lago, E.; Varela-Varela, S.; Peña-Gallego, A.; Hermida-Ramón, J. *J. Org. Chem.* **2005**, *70*, 3921–3928. (d) Birney, D. *J. Org. Chem.* **1996**, *61*, 243–251. (e) Rodríguez-Otero, J.; Cabaleiro-Lago, E. *Chem.—Eur. J.* **2003**, *9*, 1837–1843. (f) Matito, E.; Poater, J.; Duran, M.; Solà, M. *ChemPhysChem* **2006**, *7*, 111–113. (g) Chamorro, E. E.; Notario, R. *J. Phys. Chem. A* **2004**, *108*, 4099–4104. (h) López, C. S.; Faza, O. N.; Cossío, F. P.; York, D. M.; de Lera, A. R. *Chem.—Eur. J.* **2005**, *11*, 1734–1738.

(3) Duncan, J. A.; Azar, J. K.; Beathe, J. C.; Kennedy, S. R.; Wulf, C. M. *J. Am. Chem. Soc.* **1999**, *121*, 12029–12034.

10.1021/ja906679g

the *terminal* π-orbital remains intact (Figure 1d), amounting to a "non-augmented" Cope rearrangement.[4]

As part of our search for a pseudopericyclic Cope rearrangement, we initially conducted a computational study of the rearrangements of bicyclic allenes *syn*-5-propadienylbicyclo[2.1.0]-pent-2-ene (**7**) and *syn*-6-propadienylbicyclo[2.1.1]hex-2-ene (**9**) to give trienes **8** and **10**, respectively.[5] While these turned out to be the first examples of fully concerted allenyl Cope rearrangements, presumably due to the high strain that would accompany the formation of biradical intermediates, the analysis of the active space MOs showed that they were classically pericyclic, i.e., with no orbital disconnections. In addition, a recent CASSCF study of the Cope rearrangement of *cis*-1-allenyl-2-vinylcyclopropane (**11**) to triene **12** indicates that it should also be concerted and pericyclic, while the Cope rearrangements of the corresponding 4- and 5-membered ring compounds were shown to likely proceed, at least partially, through biradical intermediates.[6] Recently, we have argued that the electrocyclization of 7-aza-hepta-1,2,4,6-tetraene (**13**) to **14** is primarily pericyclic with a certain amount of pseudopericyclic character as a consequence of a secondary orbital effect involving the nitrogen lone-pair orbital, though no orbital disconnection was observed for the allenyl moiety.[2a] Birney has also recently argued that the [3,3] sigmatropic rearrangements of allyl esters are primarily pseudopericyclic.[1d]

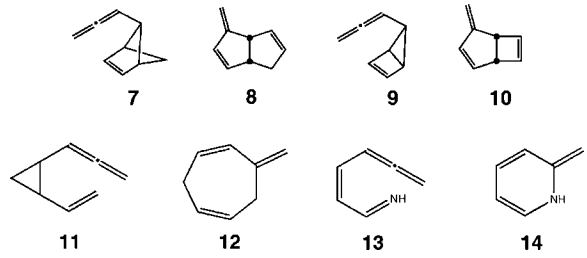

Computational Details

CASSCF calculations on all stationary points were performed using a (10,9) active space of ten electrons in nine orbitals (**17**, $\mathbf{TS_{17\rightarrow18}}$, and $\mathbf{TS_{21\rightarrow22}}$) or a (12,10) one with twelve electrons in ten orbitals (**15**, **19**, **27**, **29**, $\mathbf{TS_{15\rightarrow16}}$, $\mathbf{TS_{19\rightarrow20}}$, $\mathbf{TS_{21\rightarrow22}}$, $\mathbf{TS_{23\rightarrow24}}$, $\mathbf{TS_{25\rightarrow26}}$, $\mathbf{TS_{29\rightarrow30}}$, $\mathbf{TS_{31\rightarrow32}}$). The nine orbitals in reactant **17** consisted of the one σ and three π bonding orbitals, their antibonding counterparts, and the lone-pair orbital on nitrogen. The ten orbitals in each of the four other optimized reactants (**15**, **19**, **27**, and **29**) consisted of the one σ and three π bonding orbitals, their antibonding counterparts, and a lone-pair orbital on each of the heteroatoms, oxygen or nitrogen. In the case of reactant **15**, however, one of the π orbitals on the allene moiety was found to form an allyl system with an oxygen lone-pair as shown on page S2 of Supporting Information. [It was not convenient to locate the full active space for reactants **21**, **23**, **25**, and **31**; however, all corresponding (12,10) transition structures were successfully optimized and are discussed in the narrative and included with Supporting Information.]

Unless otherwise indicated, all calculations made use of the Gaussian 03[7a] suite of programs and the 6-31G* basis set was used throughout. Appropriate vibrational analyses were also carried out, through analytical or numerical frequency calculations, to characterize stationary points as either energy minima (reactants) or first order saddle points (transition structures) and to obtain zero-point energy differences. The concerted nature of the **15** → **16**, **17** → **18**, **19** → **20**, **21** → **22**, **23** → **24**, **25** → **26**, **27**→ **28**, **29** → **30**, and **31** → **32** rearrangements was confirmed by animation of the normal mode corresponding to the imaginary frequency of $\mathbf{TS_{15\rightarrow16}}$, $\mathbf{TS_{17\rightarrow18}}$, $\mathbf{TS_{19\rightarrow20}}$, $\mathbf{TS_{21\rightarrow22}}$, $\mathbf{TS_{23\rightarrow24}}$, $\mathbf{TS_{25\rightarrow26}}$, $\mathbf{TS_{27\rightarrow28}}$, $\mathbf{TS_{29\rightarrow30}}$, $\mathbf{TS_{31\rightarrow32}}$ (cf. Figure 3 and Supporting Information), and in the case of the novel **15** → $\mathbf{TS_{15\rightarrow16}}$ → **16** process through CASSCF/6-31G* intrinsic reaction coordinate (IRC) calculations as well. The IRC calculations were performed with Gaussian 09.[7b,8]

The three-dimensional structural representations including normal mode vectors shown in Figure 3 and in the Supporting Information, as well as the MO representations shown in Figures 1, 2, and in Supporting Information were prepared using MacMolPlt[9] with the Contour Value set to between 0.06 and 0.10.

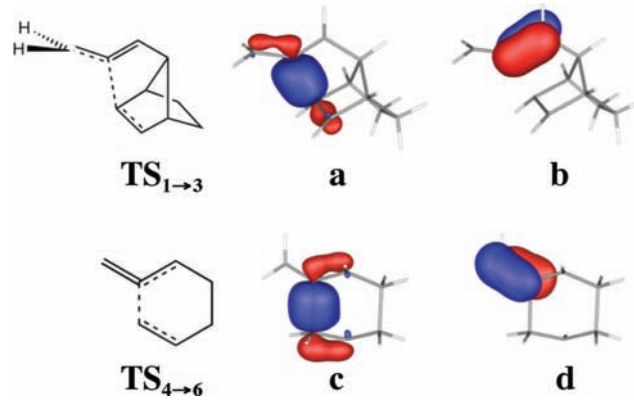

Figure 1. ChemDraw representations of $\mathbf{TS_{1\rightarrow3}}$ and $\mathbf{TS_{4\rightarrow6}}$, and selected active space $\mathbf{TS_{1\rightarrow3}}$ MOs (**a** and **b**) and $\mathbf{TS_{4\rightarrow6}}$ MOs (**c** and **d**).

Results and Discussion

We now report on CASSCF calculations that, to the best of our knowledge, reveal the first purely pseudopericyclic [3,3] sigmatropic rearrangement. Given the similarity in structure between **13**, the electrocyclization of which appears to possess at least some pseudopericyclic character, and **11**, the Cope rearrangement of which is likely concerted, and the fact that it has been surmised that electrocyclizations are more likely to exhibit pseudopericyclic character the more nucleophic and electrophilic the reacting centers,[2] we decided to search for a pseudopericyclic mechanism from among the [3,3] sigmatropic rearrangements shown in Scheme 1. Given the relative nucleophilicity/electrophilicity of the reacting centers, we might expect the **15** → **16** rearrangement to be the most pseudopericyclic and the **17** → **18** rearrangement to be the least pseudopericyclic.

Indeed, CASSCF/6-31G* calculations revealed the **15** → **16** rearrangement to be purely pseudopericyclic and the **17** → **18** and **19** → **20** ones to be classically pericyclic. Figure 2 shows structural representations of $\mathbf{TS_{15\rightarrow16}}$, $\mathbf{TS_{17\rightarrow18}}$, and $\mathbf{TS_{19\rightarrow20}}$, as well as selected active space TS MOs derived from these rearrangements. ($\mathbf{TS_{29\rightarrow30}}$ and $\mathbf{TS_{31\rightarrow32}}$ will be discussed later in this article.) Interestingly, $\mathbf{TS_{15\rightarrow16}}$ could only be optimized

(4) Hrovat, D. A.; Duncan, J. A.; Borden, W. T. *J. Am. Chem. Soc.* **1999**, *121*, 169–175.
(5) Duncan, J. A.; Spong, M. C. *J. Org. Chem.* **2000**, *65*, 5720–5727.
(6) Duncan, J. A.; Calkins, D. E. G.; Forte, L.; Delaney, F. E.; Lafortune, M. C.; Chavarha, M. Unpublished results.
(7) (a) Frisch, M. J.; et al. *Gaussian 03*, Revisions D.01 and E.01; Gaussian, Inc.: Wallingford, CT, 2004. (b) Frisch, M. J.; et al. *Gaussian 09*, Revision A.01; Gaussian, Inc.: Wallingford, CT, 2009.
(8) Improvements in Gaussian 09, over Gaussian 03, made it possible for these large active space CASSCF-level IRCs to be examined.
(9) Bode, B. M.; Gorgon, M. S. *J. Mol. Graphics Modell.* **1998**, *16*, 133–138.
(10) As depicted in Figure 2, orbitals **n** and **q** both show only a small orbital contribution at one carbon atom. However, this is just an artifact resulting from the contour level chosen to make their representations relatively consistent with the other orbitals shown in the figure.

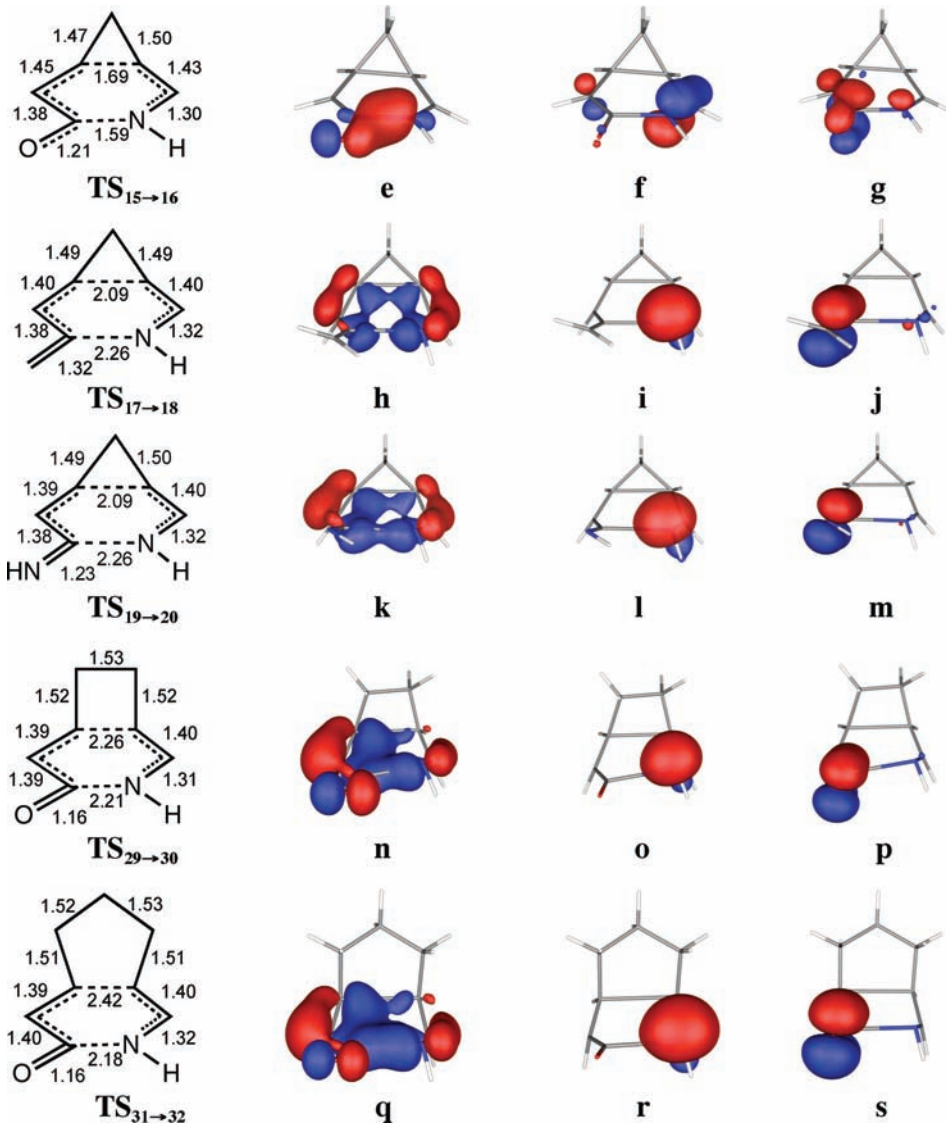

Figure 2. ChemDraw representations for $\mathbf{TS}_{15\rightarrow16}$, $\mathbf{TS}_{17\rightarrow18}$, $\mathbf{TS}_{19\rightarrow20}$, $\mathbf{TS}_{29\rightarrow30}$, and $\mathbf{TS}_{31\rightarrow32}$ with bond lengths in Angstroms, and selected active space $\mathbf{TS}_{15\rightarrow16}$ MOs (**e**, **f**, and **g**), $\mathbf{TS}_{17\rightarrow18}$ MOs (**h**, **i**, and **j**), $\mathbf{TS}_{19\rightarrow20}$ MOs (**k**, **l,** and **m**), $\mathbf{TS}_{29\rightarrow30}$ MOs (**n**, **o**, and **p**), and $\mathbf{TS}_{31\rightarrow32}$ MOs (**q**, **r**, and **s**).

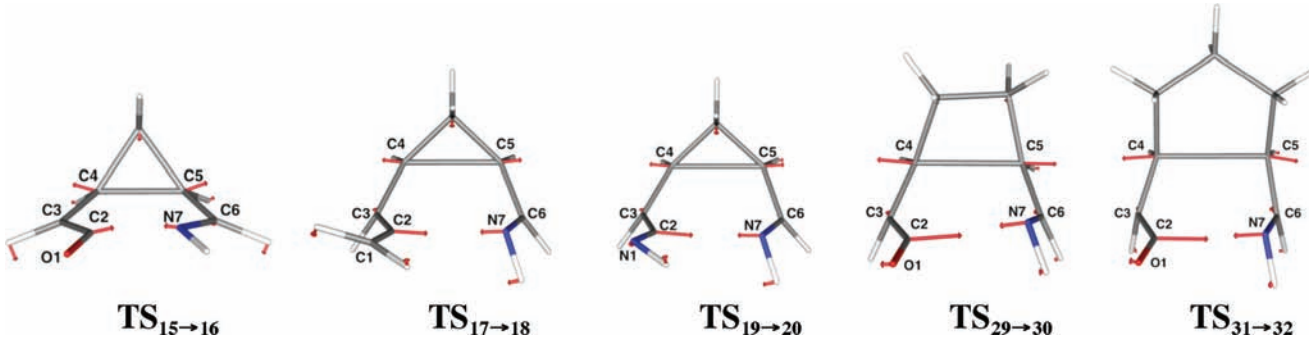

Figure 3. CASSCF/6-31G* optimized geometries for $\mathbf{TS}_{15\rightarrow16}$, $\mathbf{TS}_{17\rightarrow18}$, $\mathbf{TS}_{19\rightarrow20}$, $\mathbf{TS}_{29\rightarrow30}$, and $\mathbf{TS}_{31\rightarrow32}$. Normal mode vectors shown in red. Forming σ-bonds omitted for clarity in viewing normal mode vectors.

if a lone-pair orbital on oxygen was included in the active space. Failure to do so always resulted in either the cyclopropane σ-bond or the nitrogen lone-pair orbital being left out of the active space and instead one of the lone-pair orbitals on oxygen was used to construct a C−C−O allyl system.

Orbital **e** for $\mathbf{TS}_{15\rightarrow16}$ in Figure 2 constitutes a localized active space MO that clearly shows not only one, but two orbital disconnections—one involving the nitrogen lone-pair orbital and the other the carbonyl carbon of the ketene moiety. As in the C−C π-MOs **b** and **d** of Figure 1, orbital **f** of Figure 2 represents an imine π-MO that remains intact. In Figure 2 are also shown selected active space MOs that demonstrate how the other two rearrangements, **17** → **18** and **19** → **20**, are classically pericyclic: orbitals **h** and **k** are bonding diallyl ones and **i** and **l** are intact

Scheme 1

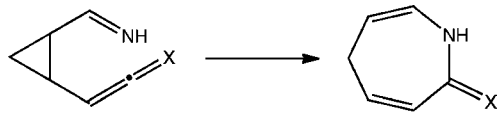

15: X=O
17: X=CH_2
19: X=NH

16: X=O
18: X=CH_2
20: X=NH

Scheme 2

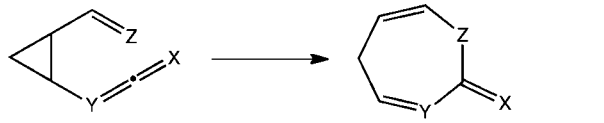

21: X=O;Y=CH;Z=CH_2
23: X=NH;Y=CH;Z=O
25: X=CH_2;Y=N; Z=O
27:X=O;Y=CH;Z=O

22: X=O;Y=CH;Z=CH_2
24: X=NH;Y=CH;Z=O
26: X=CH_2;Y=N; Z=O
28:X=O;Y=CH;Z=O

Scheme 3

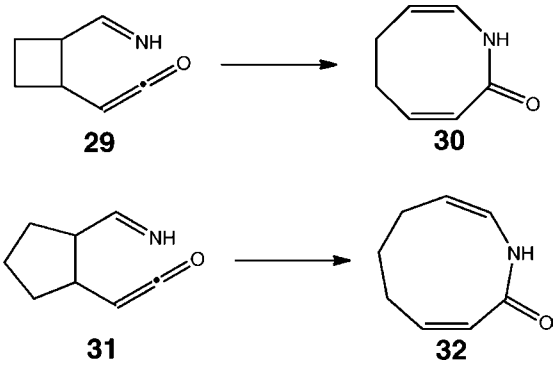

lone-pair orbitals. Moreover, among the full set of active space orbitals included for $\mathbf{TS_{17\rightarrow18}}$ and $\mathbf{TS_{19\rightarrow20}}$ in Supporting Information (pages S14 and S16, respectively) are these that constitute a full set of bonding, nonbonding, and antibonding diallyl MOs (those with occupation numbers 1.95, 1.89, 1.81, 0.19, 0.11, and 0.5 for $\mathbf{TS_{17\rightarrow18}}$ and 1.95, 1.91, 1.84, 0.17, 0.09, and 0.05 for $\mathbf{TS_{19\rightarrow20}}$) characteristic of concerted [3,3] sigmatropic rearrangements. In addition, among the active space MOs of $\mathbf{TS_{17\rightarrow18}}$ and $\mathbf{TS_{19\rightarrow20}}$ shown in Figure 2 are intact exocyclic C−CH_2 (**i**) and C−NH (**m**) bonding π-MOs respectively, comparable to orbital **d** shown in Figure 1. However, the calculated active space for $\mathbf{TS_{15\rightarrow16}}$ has no such intact exocyclic π-MO but rather a delocalized allylic π-MO, the bonding one included as orbital **g** in Figure 2. (All active space MOs are included with Supporting Information.)

Purely pseudopericyclic transition structures such as $\mathbf{TS_{15\rightarrow16}}$ appear to be rare as demonstrated by further CASSCF/6-31G* calculations that revealed the [3,3] sigmatropic rearrangements of **21**, **23**, and **25** (Scheme 2) to be classically pericyclic. Only the result obtained for the rearrangement of **27** was found in any way ambiguous. It appears to possess some pseudopericyclic character, in a way similar to that previously demonstrated for the **13** → **14** rearrangement.[2a] [Coordinates and all active space MOs for the transition structures corresponding to the rearrangements shown in Scheme 2 ($\mathbf{TS_{21\rightarrow22}}$, $\mathbf{TS_{23\rightarrow24}}$, $\mathbf{TS_{25\rightarrow26}}$, and $\mathbf{TS_{27\rightarrow28}}$) can be found in Supporting Information.]

We also studied the two rearrangements shown in Scheme 3 to evaluate the effect, if any, of increasing the ring size on the **15** → $\mathbf{TS_{15\rightarrow16}}$ → **16** rearrangement, thus far the only purely pseudopericyclic one uncovered. As shown in Figure 2, orbital analysis shows that these otherwise comparable four- and five-membered ring rearrangements are also classically pericyclic, supporting the notion that the **15** → $\mathbf{TS_{15\rightarrow16}}$ → **16** one is indeed uncommon. Orbitals **n** and **q** are bonding diallyl ones,[9] isolated nitrogen lone-pair orbitals are clearly seen in **o** and **r**, and the exocyclic C−O bonding π-MOs remain fully intact (**p** and **s**).

Figure 2 also serves to compare the bond lengths in $\mathbf{TS_{15\rightarrow16}}$, $\mathbf{TS_{17\rightarrow18}}$, $\mathbf{TS_{19\rightarrow20}}$, $\mathbf{TS_{29\rightarrow30}}$, and $\mathbf{TS_{31\rightarrow32}}$. The forming σ-bond length of 1.59 Å for $\mathbf{TS_{15\rightarrow16}}$ is exceptionally short, especially as compared to the other four transition structures. This is likely a consequence of the excellent orbital overlap that may be obtained from the two orbital disconnections as shown in orbital **e** in Figure 2. Also a general trend is observed in the breaking σ-bond lengths of the classically pericyclic transition structures. They increase from 2.09 Å in 3-membered ring cases $\mathbf{TS_{17\rightarrow18}}$ and $\mathbf{TS_{19\rightarrow20}}$ to 2.26 Å in $\mathbf{TS_{29\rightarrow30}}$, containing the 4-membered ring, and to 2.42 Å in $\mathbf{TS_{31\rightarrow32}}$, containing the 5-membered ring. This is consistent with the Hammond Postulate that predicts that the more exothermic a reaction is the earlier its transition state should be. However in the pseudopericyclic transition structure, $\mathbf{TS_{15\rightarrow16}}$, the breaking σ-bond length at 1.69 Å is exceptionally short vis-à-vis the 2.09 Å ones in the two pericyclic 3-membered ring cases $\mathbf{TS_{17\rightarrow18}}$ and $\mathbf{TS_{19\rightarrow20}}$. This is perhaps a consequence of the overall geometrical accommodation that must transpire in order to take most advantage of the orbital overlap at the orbital disconnection sites in forming the σ-bond. Finally, it is noteworthy that at 1.21 Å, the C−O bond length in $\mathbf{TS_{15\rightarrow16}}$ is considerably longer than it is in $\mathbf{TS_{29\rightarrow30}}$ and $\mathbf{TS_{31\rightarrow32}}$ (1.16 Å). This difference is likely a consequence of the C−O π-MO's participation through an orbital disconnection at the carbonyl carbon in pseudopericyclic transition structure $\mathbf{TS_{15\rightarrow16}}$, but with such participation lacking in the classically pericyclic transition structures $\mathbf{TS_{29\rightarrow30}}$ and $\mathbf{TS_{31\rightarrow32}}$ that involve no orbital disconnections.

Figure 3 displays geometrical structures representing the CASSCF/6-31G* optimized geometries for $\mathbf{TS_{15\rightarrow16}}$, $\mathbf{TS_{17\rightarrow18}}$, $\mathbf{TS_{19\rightarrow20}}$, $\mathbf{TS_{29\rightarrow30}}$ and $\mathbf{TS_{31\rightarrow32}}$, as well as the normal mode vectors (in red) for the imaginary frequencies of these transition structures.[11] In all cases, animation of these frequencies primarily shows simultaneous displacement, in opposing directions, of C4 relative to C5 and C2 relative to N7. Such motion is consistent with the normal mode vectors and argues for the concerted nature of the rearrangements associated with all five of these transition structures as well as all the other rearrangements studied. (Geometrical structures as well as normal mode vectors for all transition structures are included with Supporting Information.)

Results of intrinsic reaction coordinate (IRC) calculations for the **15** → $\mathbf{TS_{15\rightarrow16}}$ → **16** rearrangement, performed with Gaussian 09,[8] also support the concerted pathway in this novel case. The IRC was followed a short distance down each side of $\mathbf{TS_{15\rightarrow16}}$—10 points on the reactant (**15**) side and 6 points on the product (**16**) side. A plot of C2−N7 bond distance vs C4−C5 bond distance for 4 points on either side of $\mathbf{TS_{15\rightarrow16}}$ exhibited a nearly linear relationship ($R^2 = 0.999$) with a slope

(11) The diasteromer of $\mathbf{TS_{19\rightarrow20}}$ depicted in Figure 3 is the more stable one with respect to the NH on the ketenimine moiety. The alternative diastereomer (with the ketenimine N−H bond pointing outward from the imine N) was shown to have an energy 5.01 kcal/mol higher and is not included among the structures reported on in this article or in Supporting Information. Likewise, the energy of the comparable diastereomer of $\mathbf{TS_{23\rightarrow24}}$ was calculated to have an energy 8.31 kcal/mol higher than the reported one.

of −0.73 (bottom graph on page S29 of Supporting Information), showing that in the vicinity of this transition structure the overall change in the C4−C5 bond length (0.20 Å) slightly exceeded the overall change in the C2−N7 bond length (0.15 Å). The remaining 6 points on the reactant side exhibited a gradual change over to having the C2−N7 bond lengthen more than the C4−C5 bond is seen to shorten (as shown by the rather smooth upward curve in the top graph on page S29 in Supporting Information), and on the product side, the remaining 2 points are approximately collinear with the 9 exceptionally collinear ones.

We also searched for possible intermediates in all rearrangements studied, but found no evidence for any, even in the case of the novel **15** → **16** rearrangement. For example, a modified Staudinger reaction,[12] involving intramolecular nucleophilic "addition" to give a zwitterionic intermediate followed by a ${}_{\pi}4_{s} + {}_{o}2_{s}$ conrotatory electrocyclic ring-opening (as opposed to a ${}_{\pi}4_{a}$ conrotatory electrocyclic ring closure to give a β-lactam in the regular Staudinger reaction), might be considered a plausible mechanism in this case, but we found no evidence for such a zwitterionic intermediate.[13] Perhaps this is not surprising in view of the fact that we have intentionally directed our computationally expensive CASSCF-level study toward the gas phase.

One criterion often used to judge the extent of pseudopericyclicity in a rearrangement is the degree of planarity of the interacting atoms in the transition structure. It has been claimed that pseudopericyclic reactions should have far more planar transition state geometries relative to their pericyclic counterparts.[1] Indeed, this appears to be born out by our results. The latter four transition structures in Figure 3 are clearly boat-shaped as one would expect for classically pericyclic [3,3] sigmatropic rearrangements. However, the considerably more planar geometry of $\mathbf{TS_{15\rightarrow16}}$ appears to be novel for such a rearrangement. This result is also consistent with Birney's contention that rearrangements with two orbital disconnections are more likely to be pseudopericyclic than those with only one orbital disconnection.[1c]

These geometrical differences are perhaps best quantified by an examination of the relevant dihedral angles. For example, in $\mathbf{TS_{15\rightarrow16}}$ the C4−C5−C6−N7 and C2−C3−C4-C5 dihedral angles were calculated to be 19.1° and 21.2° respectively. However, for all the 3-membered ring transition structure cases that were shown by orbital analysis to be classically pericyclic ($\mathbf{TS_{17\rightarrow18}}$, $\mathbf{TS_{19\rightarrow20}}$, $\mathbf{TS_{21\rightarrow22}}$, $\mathbf{TS_{23\rightarrow24}}$, and $\mathbf{TS_{25\rightarrow26}}$), the corresponding dihedral angles were found to be much larger with ranges of 48.4−54.9° and 47.7−51.8° respectively. (Individual dihedral angles for all computed transition structures are provided in Supporting Information.) These dihedral angles are for the most part even larger in $\mathbf{TS_{29\rightarrow30}}$ and $\mathbf{TS_{31\rightarrow32}}$ containing 4- and 5-membered rings. In the case of $\mathbf{TS_{29\rightarrow30}}$, they are, respectively, 53.3° and 58.5°; and in the case of $\mathbf{TS_{31\rightarrow32}}$ 63.7° and 61.4°. The latter numbers are very comparable to the corresponding C1−C2−C3−C4 dihedral angle of 65.1°, calculated at the B3LYP/6-31G* level, for the boat-form prototypical Cope rearrangement of the hydrocarbon 1,5-hexadiene.[14] From this it might be surmised that the cyclopentane ring in $\mathbf{TS_{31\rightarrow32}}$ does little in restricting this transition structure's conformational mobility relative to the one in the acyclic 1,5-hexadiene. The lower dihedral angle values, and consequently the greater planarity observed for all the other transition structures probably arises from at least some restriction in conformation mobility that is a direct consequence of the presence of a cyclopropane moiety, and to a lesser extent the cyclobutane moiety. Thus, one cannot expect to relate the extent of pseudopericyclicity with the degree of planarity in these systems.

Fortunately, orbital analysis can serve as the principal criterion to judge pseudopericyclicity with geometrical concerns secondary. Nonetheless, as mentioned above, the one transition structure of all those studied that we consider purely pseudopericyclic i.e., $\mathbf{TS_{15\rightarrow16}}$ with dihedral angles of only 19.1° and 21.2°, is considerably more planar than the others with corresponding dihedral angles ranging from 44.0° to 63.7°. Along these same lines we do not consider the lack of full planarity of $\mathbf{TS_{15\rightarrow16}}$ to anyway detract from what we consider to be essentially a purely pseudopericyclic transition structure. As depicted in Figure 2, the MO differences between $\mathbf{TS_{15\rightarrow16}}$ and all others, which we likewise consider to be purely pericyclic in the classical sense, is striking for all the reasons already alluded to above.

As also mentioned above, however, we found one result to be ambiguous, namely the nature of $\mathbf{TS_{27\rightarrow28}}$ which we have tentatively classified as possessing only some pseudopericyclic character. If geometry were the only guide, then it would not be considered to possess much pseudopericyclic character since the dihedral angle values for C4−C5−C6−O7 and C2−C3−C4−C5 were both calculated to be 44.0°, though this is equal to or lower than any of the dihedral angle values calculated for the classically pericyclic transition structures. Nonetheless the active space MOs of $\mathbf{TS_{27\rightarrow28}}$ are not as "clean" as all the others (cf. page S24 of Supporting Information) and thus may signify a transition structure with partial pseudopericyclic character as has been considered recently by ourselves[2a] and others[1d,15] for certain rearrangement reactions. It is worth noting that when the electrophilic/nucleophilic nature of the reacting centers in $\mathbf{TS_{27\rightarrow28}}$ is considered, with its highly electrophilic ketene moiety and its reasonably nucleophilc aldehyde moiety, the **27** → $\mathbf{TS_{27\rightarrow28}}$ rearrangement might be expected to be the second most pseudopericyclic in character after the **15** → $\mathbf{TS_{15\rightarrow16}}$ one, the latter having the more nucleophilic imine moiety in addition to the ketene one.

(12) (a) Cossío, F. P.; Arrieta, A.; Sierra, M. A. *Acc. Chem. Res.* **2008**, *41*, 925–936. (b) Fu, N.; Tidwell, T. T. *Tetrahedron* **2008**, *64*, 10465–10496.

(13) In this regard it is worth considering that a zwitterionic intermediate between $\mathbf{TS_{15\rightarrow16}}$ and **16** might open without a barrier which would mean the reaction "turns a corner" on the PES as Birney et al. has proposed for the Diels-Alder reaction of an electron deficient pyridazine with an ynamine: Sadasivam, D. V.; Prasad, E.; Flowers, II, R. A.; Birney, D. M. *J. Phys. Chem. A* **2006**, *110*, 1288−1294. However, our IRC data, discussed above and included with Supporting Information (page S29), appears to show that $\mathbf{TS_{15\rightarrow16}}$ is headed toward product **16** with rather comparable C4−C5 bond breaking and C2−N7 bond making. Thus it doesn't appear to be on a trajectory to a zwitterionic intermediate with relatively short C4−C5 and C2−N7 bonds, which might open to **16** via C4−C5 bond cleavage without a barrier.

(14) Wiest, O.; Black, K. A.; Houk, K. N. *J. Am. Chem. Soc.* **1994**, *116*, 10336–10337.

(15) Birney has recently reported on the [3,3] sigmatropic rearrangement of diastereomers of 1-methyl-2-butenyl acetate, arguing that the transition structures that arise from mixing of pericyclic and pseudopericyclic electronic states are primarily pseudopericyclic in character. The dihedral angle value for the one comparable to C4−C5−C6−O7 in $\mathbf{TS_{27\rightarrow28}}$ was calculated at the B3LYP/6-31G** level to be 43.6°. This is remarkably similar to the 44.0° dihedral angle calculated for $\mathbf{TS_{27\rightarrow28}}$ which we also consider to possess a certain amount of pseudopericyclic character.

Another criterion often used to evaluate pseudopericyclicity is activation energies. Indeed the CASSCF/6-31G* activation enthalpy for **15** → **TS$_{15\rightarrow16}$** was found to be lower (19.4 kcal/mol) than those for **17** → **TS$_{17\rightarrow18}$** (26.2 kcal/mol), **19** → **TS$_{19\rightarrow20}$** (22.8 kcal/mol), and **29** → **TS$_{29\rightarrow30}$** (33.1 kcal/mol) as would be expected for a pseudopericyclic reaction.[16]

If desired, an experimental test of the uniqueness of our computed transition structure **TS$_{15\rightarrow16}$** might be built around the method used by Schulz in developing an antibody catalyst for the oxy-Cope rearrangement of a hydroxycyclohexane mimic,[17] though this would be no trivial undertaking. Since the C_6H_7NO **TS$_{15\rightarrow16}$** is relatively planar, with exceptionally short breaking and forming σ bonds, it has a very similar geometry to the corresponding C_6H_9NO δ-lactam 3-azabicyclo[4.1.0]heptan-4-one, a known compound. Thus, with a linker attached to its nitrogen atom, this δ-lactam might serve as a mimic in the present case. Then if one of the antibodies raised against this mimic substantially catalyzed the **11** to **12**, allegedly pseudopericyclic rearrangement, it could be argued that the actual transition state has the unusual, relatively planar, tight geometry predicted by our calculations.

Conclusions

The novel purely pseudopericyclic nature of **TS$_{15\rightarrow16}$**, involving two orbital disconnections in a cyclic array of interacting orbitals, versus the classically pericyclic nature of **TS$_{17\rightarrow18}$**, **TS$_{19\rightarrow20}$**, **TS$_{21\rightarrow22}$**, **TS$_{23\rightarrow24}$**, **TS$_{25\rightarrow26}$**, **TS$_{29\rightarrow30}$**, and **TS$_{31\rightarrow32}$** is attributed to the following: (1) the greater nucleophilicity/electrophilicity of the reacting centers in **TS$_{15\rightarrow16}$**, (2) its highly limited conformational mobility due to the presence of the 3-membered ring, and (3) the tendency of **TS$_{15\rightarrow16}$** to form an allyl system using a lone-pair orbital on the oxygen atom. The relatively planar, tight geometry calculated for **TS$_{15\rightarrow16}$** (cf., Figure 3) is consistent with the appearance and participation of the active space orbitals (cf., parts **e**, **f**, and **g** of Figure 2) and highly unusual for a Cope-type transition structure. Though transition state geometry can apparently aid in assessing the degree of pseudopericyclicity of certain rearrangements, we consider it secondary to an active space orbital analysis. Nor does it appear that a transition structure need be completely planar, or even nearly so, to be purely pseudopericyclic. Finally, given the number of potentially pseudopericyclic rearrangements examined in this study by the CASSCF computational method that were shown to be classically pericyclic, pseudopericyclic reactions may be rarer than first thought and may indeed require not just one but two orbital disconnections to be purely so.

Acknowledgment. Support for this work from the John S. Rogers Science Research Program of Lewis & Clark College is appreciated. We especially thank Mr. Chris Stevens, Director of Network and Technical Services at Lewis & Clark, for his tireless technical assistance and Dr. David Hrovat of the University of North Texas for his extremely helpful advice in performing calculations over the past 13 years. Finally, we thank Dr. Douglas J. Fox, Technical Support, Gaussian, Inc., for running the CASSCF-level IRC calculations for us using Gaussian 09.[7b]

Supporting Information Available: Complete ref 7. CASSCF/6-31G* optimized geometries and structures, including normal mode vectors, for transition structures. All active space MOs and their occupation numbers for **15**, **17**, **19**, **27**, **29**, **TS$_{15\rightarrow16}$**, **TS$_{17\rightarrow18}$**, **TS$_{19\rightarrow20}$**, **TS$_{21\rightarrow22}$**, **TS$_{23\rightarrow24}$**, **TS$_{25\rightarrow26}$**, **TS$_{27\rightarrow28}$**, **TS$_{29\rightarrow30}$**, and **TS$_{31\rightarrow32}$**. IRC bond length analysis. This material is available free of charge via the Internet at http://pubs.acs.org.

JA906679G

(16) While these CASSCF energies do not fully recover dynamic electron correlation, they should reflect the relative enthalpy of activation differences among these reactions. We have had difficulty obtaining reliable CASPT2 or CASSCF-MP2 energies though all calculations point to a very low activation enthalpy for **15** → **TS$_{15\rightarrow16}$**. Also, we were unable to calculate the activation enthalpy for **31** → **TS$_{31\rightarrow32}$** as we were unsuccessful in locating the correct active space for reactant **31**.

(17) (a) Braisted, A. C.; Schultz, P. G. *J. Am. Chem. Soc.* **1994**, *116*, 2211–2212. (b) Ulrich, H. D.; Mundorff, E.; Santarsiero, B. D.; Driggers, E. M.; Stevens, R. C.; Schultz, P. G. *Nature* **1997**, *389*, 271–275.